STRANGENESS PRODUCTION IN HEAVY-ION COLLISIONS AT THE NA61/SHINE EXPERIMENT*

Yuliia Balkova

for the NA61/SHINE Collaboration

University of Silesia, Bankowa 12, 40-007 Katowice, Poland

Received 9 November 2023, accepted 22 December 2023, published online 24 April 2024

The study of strangeness production in heavy-ion collisions has been an active research area for several decades, as it provides crucial insights into the studies of the properties of strongly interacting matter. The NA61/SHINE experiment at CERN's Super Proton Synchrotron (SPS) is one of the leading experiments in this field, thanks to systematic studies of hadron production in a wide range of collision energies and system sizes. The paper emphasizes the importance of measuring the strangeness production for the discussion concerning the onset of deconfinement. The latest results from the NA61/SHINE experiment on strangeness production in heavy-ion collisions are discussed and compared to available world data and selected theoretical models.

DOI:10.5506/APhysPolBSupp.17.3-A20

1. Introduction

The properties of quark–gluon plasma (QGP) remain a key research topic in high-energy heavy-ion physics. This deconfined state of strongly interacting matter is believed to have existed in the very early Universe ($\sim \mu$s after the Big Bang), which is a strong motivation to recreate the state in controlled laboratory conditions. As a result, multiple theoretical and experimental efforts have been made to shed light on the phase diagram of strongly interacting matter. Theoretical predictions of the phase diagram are summarized in Fig. 1.

The significance of studying the strangeness production [1] was initially shown as its enhancement may indicate the occurring phase transition from hadron gas to quark–gluon plasma. The Statistical Model of Early Stage (SMES) [2] particularly predicted a sharp maximum (commonly referred to

* Presented at the XXXVII Mazurian Lakes Conference on Physics, Piaski, Poland, 3–9 September, 2023.

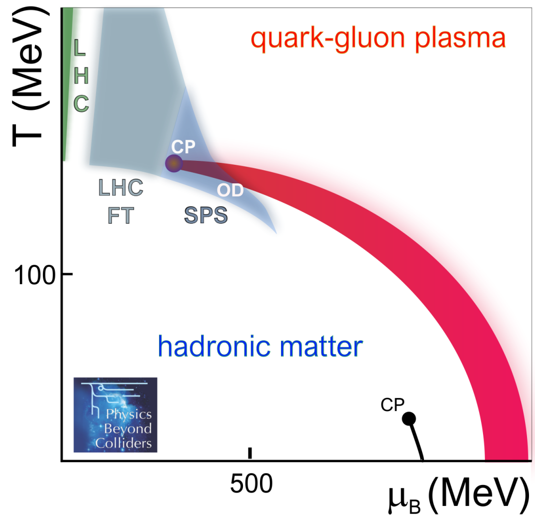

Fig. 1. Theoretical predictions of the phase diagram of strongly interacting matter. CP is the critical point of the nuclear liquid-gas phase transition. The shaded band shows the 1st order phase boundary between the hadron and quark–gluon plasma phase, which is expected to end in a critical endpoint CP [3].

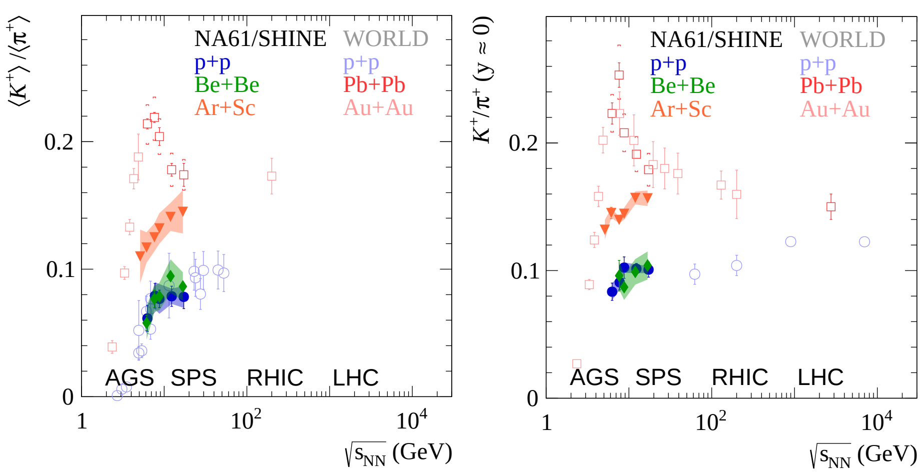

Fig. 2. $\langle K^+\rangle\,/\,\langle\pi^+\rangle$ ratio in full 4π phase space (left) and the K^+/π^+ ratio at mid-rapidity (right) as a function of collision energy for $p+p$, Be+Be, Ar+Sc, and Pb+Pb/Au+Au collisions (the references for used data are available in captions of Figs. 32 and 33 of [4]).

as “horn”) in strangeness-to-entropy ratio, which was experimentally validated [5] as shown in Fig. 2. Commonly, the strangeness production in this ratio is expressed through the experimentally measured multiplicity of positively charged kaons, although it is ideally preferable to encompass the production of other strange hadrons as well.

2. NA61/SHINE detector

NA61/SHINE is a fixed-target experiment, which is located at the H2 beamline of the CERN North Area [6] at the CERN Super Proton Synchrotron. It is the experiment aiming at investigating the onset of deconfinement with a focus on the measurement of hadron production in a wide range of collision energies and system sizes. The schematic layout of the NA61/SHINE detector is shown in Fig. 3.

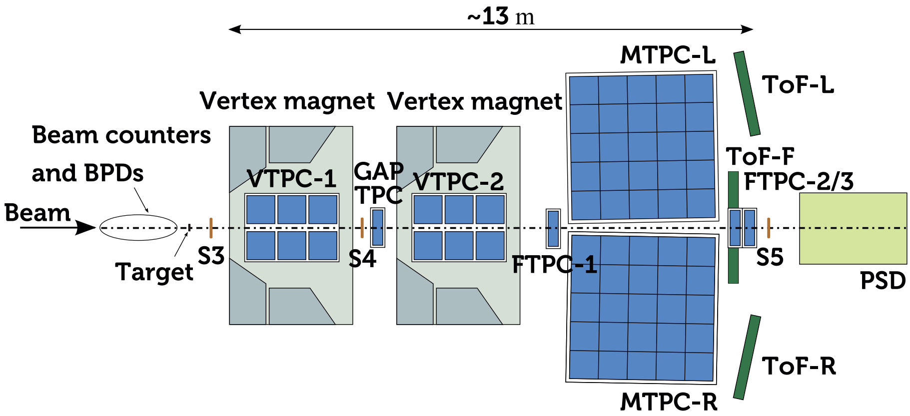

Fig. 3. Schematic view of the NA61/SHINE detector system.

The beam position detectors, which are situated upstream of the target, provide information on the incoming beam’s composition and trajectory. Particle identification is conducted using measurements from a combination of Time Projection Chambers (TPCs), two of which are positioned within the magnetic field generated by superconducting dipole magnets and Time-of-Flight detectors. In particular, the particle identification performed in the TPCs is based on measurements of the specific energy loss ($\mathrm{d}E/\mathrm{d}x$) in the chamber gas. The Projectile Spectator Detector (PSD), a precision forward calorimeter, measures the energy around the beam direction, which in nucleus–nucleus reactions is primarily a measure of the number of the projectile spectator (non-interacted) nucleons and is thus related to the violence (centrality) of the collision.

3. Results

Preliminary measurements of the rapidity spectrum (in the center-of-mass frame) and the mean multiplicity of Λ baryons produced in the 0–10% most central Ar+Sc collisions at $75A$ GeV/c ($\sqrt{s_{NN}} = 11.9$ GeV) are presented. The detailed description of the analysis workflow can be found in [7]. One-dimensional transverse momentum spectra have been fitted with an exponential function

$$f(p_T) = A \cdot p_{\mathrm{T}} \cdot \exp \frac{\sqrt{p_{\mathrm{T}}^2 + m_\Lambda^2}}{T}\,, \tag{1}$$

where T is the inverse slope parameter, m_Λ denotes Λ rest mass, and A is a normalization factor, T and A are fit parameters. It is done to extrapolate spectra to the unmeasured p_{T} region. The resulting one-dimensional rapidity spectrum is shown in Fig. 4 alongside the prediction of the EPOS 1.99 model [8, 9], which underestimates the Λ yields by 20–25%.

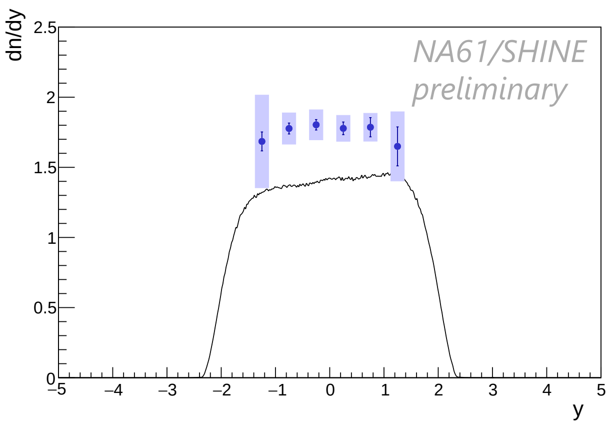

Fig. 4. Rapidity spectrum of Λ baryons produced in 0–10% most central Ar+Sc collisions at $75A$ GeV/c (in the center-of-mass frame). Statistical uncertainties are shown as vertical bars, and systematic ones are denoted as shaded boxes. The spectrum is compared with EPOS 1.99 model prediction, depicted as a black line [8, 9].

The mean multiplicity $\langle\Lambda\rangle$ is calculated from the sum of measured data points scaled by the ratio between measured and unmeasured regions from the EPOS model. The obtained mean multiplicity of Λ baryons equals 6.44 $\pm$ 0.24 (stat.) $\pm$ 1.10 (sys.).

The $\langle \Lambda \rangle / \langle \pi^+ \rangle$ ratio is then compared for different collision systems in Fig. 5 using the numerical results for pion multiplicity from Ref. [4]. One can see that it shows a qualitatively similar trend to that observed for $\langle K^+ \rangle / \langle \pi^+ \rangle$ ratio [4].

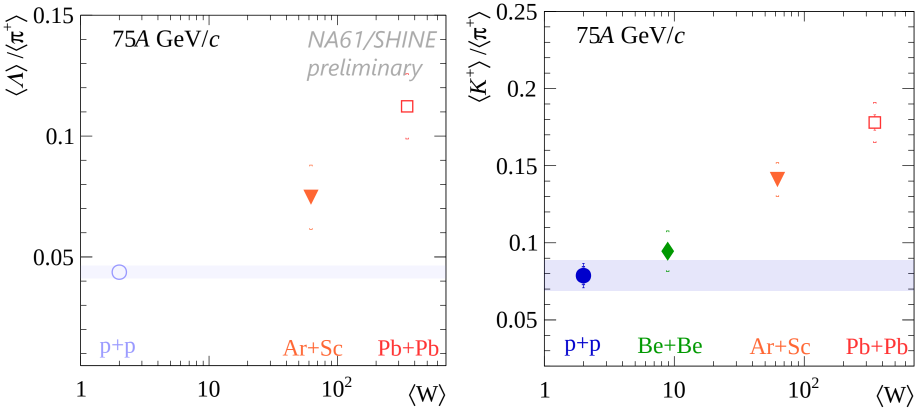

Fig. 5. The system size dependence of $\langle \Lambda \rangle / \langle \pi^+ \rangle$ ratio (left) and the $\langle K^+ \rangle / \langle \pi^+ \rangle$ ratio [4] (right) in full 4π phase space. Statistical uncertainties are shown as bars, and systematic ones are denoted with square braces. The shaded band shows the total uncertainty of the $p + p$ result. The numerical data needed to obtain $p + p$ and Pb+Pb points at similar energies were taken from Refs. [5, 10–12].

This work was supported by the funds granted under the Research Excellence Initiative of the University of Silesia in Katowice and by the Polish Ministry of Education and Science (contract No. 2021/WK/10).

REFERENCES

[1] J. Rafelski, B. Müller, *Phys. Rev. Lett.* **48**, 1066 (1982); *Erratum ibid.* **56**, 2334 (1986).

[2] M. Gaździcki, M.I. Gorenstein, *Acta Phys. Pol. B* **30**, 2705 (1999).

[3] M. Gazdzicki, M. Gorenstein, P. Seyboth, *Acta Phys. Pol. B* **42**, 307 (2011).

[4] NA61/SHINE Collaboration (H. Adhikary *et al.*), submitted to *Eur. Phys. J. C*.

[5] NA49 Collaboration (S.V. Afanasiev *et al.*), *Phys. Rev. C* **66**, 054902 (2002).

[6] NA61/SHINE Collaboration (N. Abgrall *et al.*), *J. Instrum.* **9**, P06005 (2014).

[7] NA61/SHINE Collaboration (Y. Balkova), *Frascati Phys. Ser.* **72**, 60 (2022).

[8] K. Werner, *Nucl. Phys. Proc. Suppl.* **175–176**, 81 (2008).

[9] T. Pierog *et al.*, *Phys. Rev.* **C 92**, 034906 (2015).
[10] V.V. Ammosov *et al.*, *Nucl. Phys. B* **115**, 269 (1976).
[11] M. Gaździcki, D. Röhrich, *Z. Phys. C* **65**, 215 (1995).
[12] NA49 Collaboration (C. Alt *et al.*), *Phys. Rev. C* **78**, 034918 (2008).